

# Monte Carlo simulations of phase transitions of systems in nanoscopic confinement

Kurt Binder <sup>a,\*</sup>, Jürgen Horbach <sup>a</sup>, Andrey Milchev <sup>b</sup>, Marcus Müller <sup>c</sup>, Richard Vink <sup>d</sup>

<sup>a</sup>*Institut für Physik, Johannes Gutenberg Universität, Mainz, 55099 Mainz, Staudinger Weg 7, Germany*

<sup>b</sup>*Institut for Physical Chemistry, Bulgarian Academy of Sciences, 1113 Sofia, Bulgaria*

<sup>c</sup>*Institut für Theoretische Physik, Universität Göttingen, Friedrich-Hund-Platz 1, 37077 Göttingen, Germany*

<sup>d</sup>*Institut für Theoretische Physik II, Universität Düsseldorf, Universitätsstr. 1, 40225 Düsseldorf, Germany*

---

## Abstract

When simple or complex fluids are confined to ultrathin films or channels or other cavities of nanoscopic linear dimensions, the interplay of finite size and surface controls the phase behavior, and may lead to phase transitions rather different from the corresponding phenomena in the bulk. Monte Carlo simulation is a very suitable tool to clarify the complex behavior of such systems, since the boundary conditions providing the confinement can be controlled and arbitrarily varied, and detailed structural information on the inhomogeneous states of the considered systems is available. Examples used to illustrate these concepts include simple Ising models in pores and double-pyramid-shaped cavities with competing surface fields, where novel types of interface localization-delocalization phenomena occur accompanied by “macroscopic” fluctuations, and colloid-polymer mixtures confined in slit pores. Finite size scaling concepts are shown to be a useful tool also for such systems “in between” the dimensionalities.

*Key words:* phase transition; nanoscopic confinement; Monte Carlo simulation

---

## 1. Introduction

Nanososcopic confinement of fluids and solids has received longstanding attention in condensed matter physics and materials science, and is particularly relevant for nanotechnology (“lab on a chip”, etc.). Such “nanosystems” are in between bulk matter and single atoms or molecules. As a consequence, finite size and surface effects are important, all physical properties are often rather inhomogeneous, and strong fluctuations may occur.

Analytical theories (typically of the “mean field”-type) are in trouble when dealing with such systems. Computer simulation is the method of choice:

one always deals with a nanosystem (containing typically  $10^2$  to  $10^6$  particles only); when describing bulk matter one normally needs the (physically artificial) periodic boundary conditions. However, for condensed matter under confinement, the confining walls and the forces they exert are an explicit part of the simulated model. In experiment, these boundary conditions due to a wall often are incompletely known, and subject to unwanted “dirt effects”. In a simulation boundary effects can be perfectly controlled, forces due to the boundaries can be varied at will. Ideal conditions can be created, that are difficult to realize in experiments. Therefore, simulations are ideal to elucidate the novel physical phenomena, that nanoscopic confinement can cause. The insight thus gained is helpful to interpret the more complex phenomena that occur in the real world.

The “leitmotif” of this paper focuses on novel phe-

---

\* Corresponding author.

*Email address:* kurt.binder@uni-mainz.de (Kurt Binder).

nomena due to surface effects on ordering phenomena and phase transitions, in the context of interfacial effects between coexisting phases. Competition between surface effects due to the walls of a container and interfacial effects may arise for applications such as nanotubes for gas storage (depending on the boundary conditions, the liquid may either condense uniformly at the walls or only partially – one may choose conditions that part of the walls favor the liquid and another part favors the gas). For separation of binary (AB) mixtures in nanoscopic cavities, selective adsorption of one component at (part of) the walls may occur. However, these application aspects are not within our focus. We rather concentrate on the simulation techniques to deal with such problems, and the corresponding computational needs.

## 2. A new type of phase transition: The Ising model in a bipyramid geometry

The new phenomena due to competition between surface and interfacial effects are easily exemplified by the Ising model, with ferromagnetic nearest neighbor exchange  $J(> 0)$  between spins  $S_i (= \pm 1)$  at lattice sites  $i$ , allowing also for a bulk field  $H$  and a surface field ( $\pm H_s$ ) that acts on the spins in the surface planes only. So the Hamiltonian that is studied is

$$\mathcal{H} = -J \sum_{\langle i,j \rangle \text{bulk}} S_i S_j - J_s \sum_{\langle i,j \rangle \text{surfaces}} S_i S_j - H \sum_i S_i - H_s \sum_{i \in W_1} S_i + H_s \sum_{i \in W_2} S_i. \quad (1)$$

Here we take  $J_s \neq J$  if both spins  $S_i, S_j$  are in the surface layers, and  $W_1$  denote the upper four triangular surfaces of the bipyramid (Fig. 1), while  $W_2$  stands for the lower four surfaces [1,2]. While such models with thin film geometry and uniform sign of the surface field are standard for surface critical phenomena [3,4] and capillary condensation [5–8], competing boundary fields lead to interface localization-delocalization transitions [9,10]. The Ising model is isomorphic to a lattice gas model for the liquid-vapor transition (spin down means a cell is taken by a fluid particle while spin up means the cell is empty) or for a binary (A,B) alloy, respectively.

Since in the limit where  $L$  diverges the spontaneous magnetization in Fig. 1 appears discontinuously one might interpret this transition as a standard first order transition, but actually it is not, it

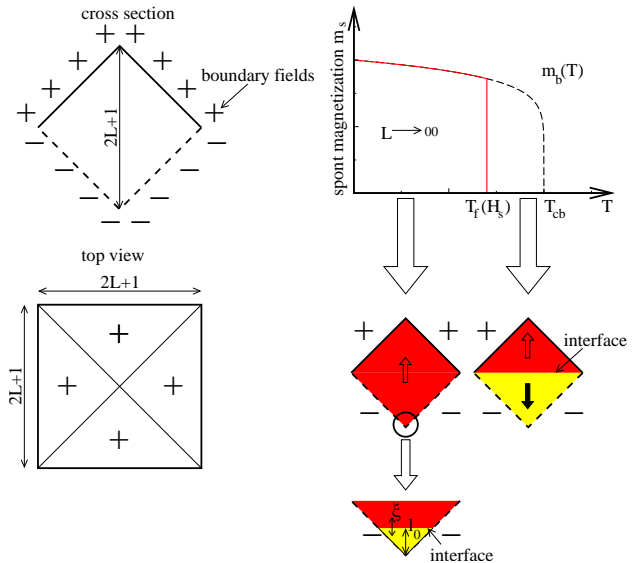


Fig. 1. Ising ferromagnet on a simple cubic lattice whose surfaces form a bipyramid (left) and resulting phase transitions in the limit where the linear dimension  $L$  diverges (right), plotting the spontaneous magnetization  $m_s(T)$  versus temperature  $T$ . Signs (+, -) along the cross section of the bipyramid (left upper part) or on the triangular projections of the surfaces in the top view (left lower part) refer to the surface field,  $\pm H_s$ . The basal plane of the bipyramid is taken to be the  $(x, y)$  plane of the lattice. Measuring lengths in units of the lattice spacing, each pyramid takes  $L$  planes (with a single spin in the pyramid top), so the total linear dimension of the bipyramid is  $2L + 1$  (the extra lattice plane accounts for the basal plane common to both pyramids). For  $T_f(H_s) < T < T_{cb}$ , a spontaneous magnetization equal to that of a bulk system,  $m_b(T)$ , occurs within two oppositely oriented domains of equal size, so the total magnetization  $m_s(T)$  of the bipyramid remains zero. At  $T < T_f(H_s)$ , however, the interface has moved towards one of the corners, and now  $m_s(T) = m_b(T)$ . The double arrow in the magnified region indicates that the local fluctuations of the interface between the domains extend over a correlation range  $\xi_{\perp}$ .

rather is a limiting case of second order transition. At a 2<sup>nd</sup> order transition, the susceptibility  $\chi$  (defined as  $\chi = (\partial m(T, H)/\partial H)_T$  for  $H \rightarrow 0$ ) diverges,

$$\chi = \Gamma(L)(T - T_f(H_s))^{-\gamma}, \quad L \rightarrow \infty, \quad (2)$$

where  $\gamma$  is a critical exponent, and  $\Gamma(L)$  the “critical amplitude” [11]. Eq. (2) holds for the model in Fig. 1, but there is one anomalous feature: normally,  $\Gamma(L \rightarrow \infty) = \Gamma_{\infty}$  (a finite constant), while here [1,2]  $\Gamma(L) \propto L$ . Similarly, also the jump of  $m_s(T)$  at  $T_f(H_s)$  from  $m_b(T)$  to zero comes about by a diverging amplitude  $B(L)$  in the relation  $m_s(T) = B(L)(1 - T/T_f(H_s))^{\beta}$ , where  $\beta$  is the order parameter exponent [1,2]. However, in a system which is finite in all its linear dimensions no sharp phase transition occurs, but rather

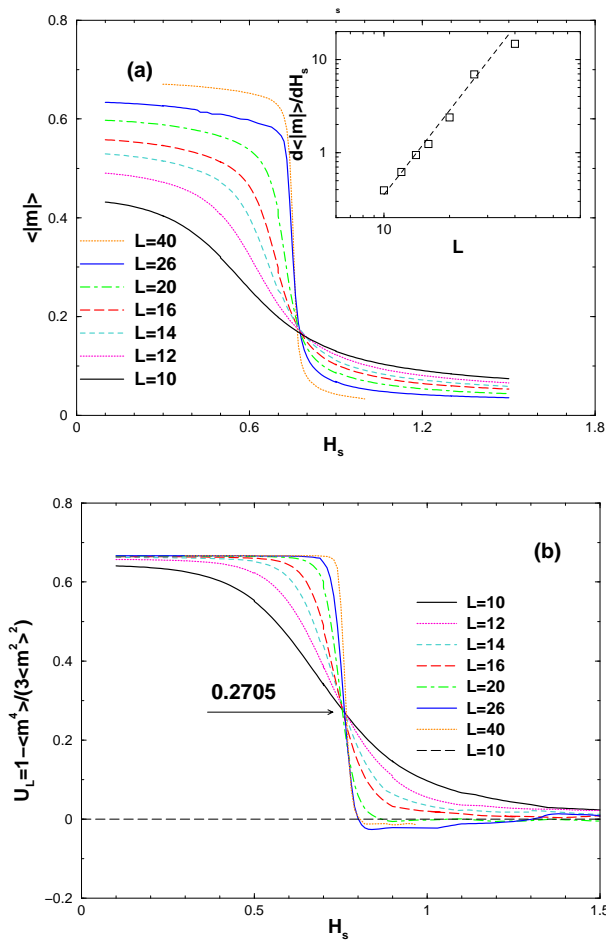


Fig. 2. (a) Plot of the absolute value  $\langle |m| \rangle$  of the magnetization per spin of the Ising bipyramid versus the surface magnetic field  $H_s$ , for  $k_B T/J = 4.0$ ,  $H = 0$ ,  $J_s/J = 0.5$ , and various linear dimensions  $L$  in the range  $10 \leq L \leq 40$ . Inset shows a log-log plot of the slope at the common intersection point vs.  $L$ . The broken straight line indicates the theoretical value [(2), see Ref. 2] of this slope. (b) Cumulants  $U_L$  [Eq. (3)] plotted vs.  $H_s$ , for various  $L$ . The arrow indicates the theoretical value [17] of the universal cumulant intersection point. All lengths are measured in units of the lattice spacing, and fields and temperatures in units of  $J$ .

the transition is rounded [12–14]. The results (Fig. 2) nicely illustrate this fact [2]. Rather than varying  $T$  at fixed  $H_s$  near  $T_f(H_s)$  {Fig. 1} it is more convenient to vary  $H_s$  at fixed  $T$  { $H_{sc}(T)$  is the inverse function of  $T_f(H_s)$  in the  $(H_s, T)$  plane}. The chosen temperature is about 12% below the bulk critical temperature ( $k_B T_{cb}/J \approx 4.51$  [16]). To locate the transition in the limit  $L \rightarrow \infty$ , the cumulant intersection method [14,15] is used, with  $U_L$  being defined as

$$U_L = 1 - \langle m^4 \rangle / [3\langle m^2 \rangle^2]. \quad (3)$$

The critical point must occur at the common intersection point of all the curves in Fig. 2b), from which we can read off  $H_{sc}(T) \approx 0.76$  (putting  $J \equiv 1$ ,  $k_B = 1$ ). There are two unusual features in Fig. 2: also the curves for  $\langle |m| \rangle$  intersect at  $H_{sc}(T)$ ; and the intersection point  $U^* = U_L(H_{sc}) = 0.2705$  is the value predicted from the Landau-theory of phase transitions [17]. Both features can be understood, concluding from the theory of cone filling [18] that the height  $\ell_0$  of the interface above the lower corner (and hence the magnetization  $m$  of the bipyramid) is the dominating variable. One arrives [1,2] at a Landau-like theory which implies for the distribution function of the magnetization  $P_L(m)$  in the volume  $V$  of the bipyramid

$$P_L(m) \propto \exp[-V f_L(m)/k_B T], \quad V = 8L^3/3 \quad (4)$$

with a free energy density  $f_L(m)$  [note  $t = (H_s - H_{sc})/H_{sc}$ ]

$$f_L(m) = r_0 t m^2 / (2L) + u m^4 / (4L^3) - H m, \quad (5)$$

where  $r_0$ ,  $u$  are phenomenological coefficients. In the standard Landau-theory in the bulk no  $L$ -dependence of  $f_L(m)$  would occur at all. From Eq. (5) one recovers Eq. (2) with  $\Gamma(L) \propto L$ , and  $\gamma = 1$ . At the transition ( $t = 0$ ) for  $H = 0$  from the distribution the  $L$ -dependence has completely canceled out,

$$P_L(m) \propto \exp[-2um^4 / (3k_B T)] \quad (6)$$

Fig. 3 shows evidence for this anomalous behavior: Eq. (6) implies that the range over which  $m$  fluctuates remains macroscopic, it does not narrow down as  $L \rightarrow \infty$ . This is very different from standard second order transitions (the range over which  $P_L(m)$  is nonzero decreases as  $L^{-\beta/\nu}$ ,  $\nu$  being the correlation length exponent. At a first order transition, we have for  $L \rightarrow \infty$  a distribution with three delta functions,  $P_L(m) \propto \delta(m - m_b) + \delta(0) + \delta(m + m_b)$ .

From Figs. 2, 3 and a detailed finite size scaling analysis [2] it is evident that systematic corrections to the asymptotic scaling are present (e.g., in Fig. 3 the surface fields chosen deviate systematically from  $H_{sc}$ ). Thus, large lattices would be desirable but this was not possible, due to pronounced critical slowing down. When one approaches  $H_{sc}$ , the interface in the basal plane exhibits very slow fluctuations. Cluster algorithms [16,19] which reduce critical slowing down near  $T_{cb}$  and allow the study of larger systems

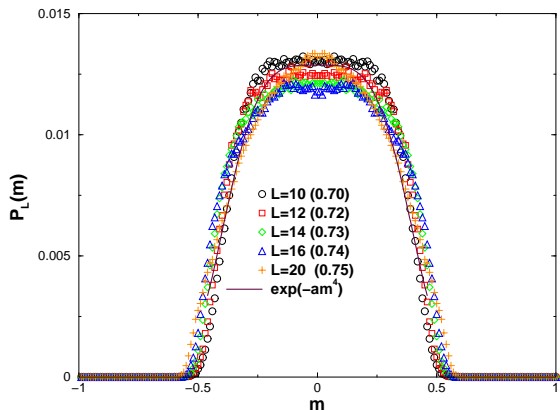


Fig. 3. Probability distribution  $P_L(m)$  of the magnetization  $m$  of Ising bipyramids for  $k_B T/J = 4$ ,  $J_s/J = 0.5$ ,  $H = 0$  and various choices of  $L$  with accompanying choices of  $H_s/J$  for which a flat variation of  $P_L(m)$  near  $m = 0$  was expected (these choices are quoted in the figure). Full curve shows the theoretical variation, from Eq. (6),  $P_L(m) \propto \exp(-am^4)$ , with  $a = 2u/3k_B T = 30.4$ .

are not useful here, since  $T$  is distinctly below  $T_{cb}$ , and also the large value  $H_{sc}$  prevents their application. Thus, the standard single spin flip Metropolis algorithm [19] had to be used! Also the Wang-Landau algorithm sampling the energy density of states would be very difficult here, most of the internal energy here is due to the spins in the bulk, while the transition is controlled by a subtle balance of surface- and interfacial energies. In fact, if the interface is at a height  $\ell_0$  above the bottom (Fig. 1) far below the basal plane, the free energy difference relative to a state with no interface is

$$\Delta F_s = 4\ell_0^2 \sigma + 8\ell_0 \sigma_{\text{line}} - 4\sqrt{2}\ell_0^2 f_s(H_s) \quad (7)$$

Here  $\sigma$  is the interfacial free energy per unit area between coexisting domains in the bulk,  $\sigma_{\text{line}}$  is the “line tension” (free energy cost of the line where the interface hits the surface planes, per unit length [20]), and  $f_s(H_s)$  is the surface free energy difference between domains oriented parallel and antiparallel to the surface field. Geometrical factors in Eq. (7) are for the opening angle  $\alpha = 45^\circ$  of the bipyramid. Using thermodynamic integration [2,19], Eq. (7) was verified: For  $H_s \leq H_{sc}$ , we expect  $f_s(H_s) = f_s(H_{sc}) + (H_s - H_{sc})f'_s$ , and hence  $\Delta\sigma/J$  for  $L \rightarrow \infty$  and  $H_s$  near  $H_{sc}$  should be a straight line, which intersects  $\sigma/J$  (which is independently known [21] with high accuracy) precisely at  $H_{sc}$ . The resulting estimate for  $H_{sc}$  (Fig. 4) agrees with the finite size scaling estimate (Fig. 2).

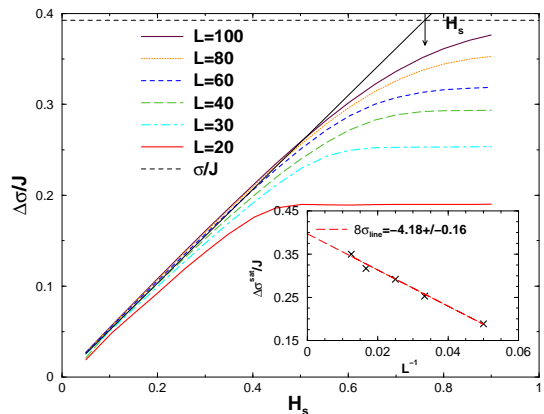


Fig. 4. Surface free energy difference  $\Delta\sigma(H_s)/J$  plotted vs. surface magnetic field  $H_s$ , as obtained from the surface magnetization  $M_s$  via thermodynamic integration [2],

$$\Delta\sigma = \int_{-H_s}^{H_s} M_s(H'_s) dH'_s.$$

Linear dimensions  $L$  from  $L = 20$  to  $L = 100$  are used, as indicated in the figure. The full straight line shows the result [2] of an extrapolation to  $L \rightarrow \infty$ . Broken horizontal straight line marks the value [21] of the interface tension  $\sigma/J$  of the Ising model at  $k_B T/J = 4$ . The inset shows the extrapolation of the apparent plateau values (reached at  $H_s = 0.9$ ) of  $\Delta\sigma/J$  plotted vs.  $L^{-1}$ . Dashed straight line in the inset represents the equation  $\Delta\sigma/J = \sigma/J + 8\sigma_{\text{line}}/L$ , the value of  $8\sigma_{\text{line}}$  is quoted in the figure. Arrow in the main part indicated the value of  $H_{sc}$ .

Finally, another type of transition with a discontinuous behavior as shown in Fig. 1 occurs for an elongated pore of square ( $L \times L$ ) cross section, having a length  $L_{\parallel} \gg L$ . Again we apply competing surface fields at the walls (the left upper part of Fig. 1 would be a sketch of the pore cross section). Now the discontinuous behavior, resulting in a particular limit (namely  $L \rightarrow \infty$ ,  $L_{\parallel} \rightarrow \infty$  with  $L^3/L_{\parallel} = \text{const}$  [22,23]), is not due to divergent amplitudes (as in Eqs. (4), (5)) but by a vanishing exponent ( $\beta = 0$ ) [22,23]. In this case nontrivial long wave length fluctuations of the interface occur in the “long” direction. Hence  $P_L(m)$  at the transition differs from Eq. (6), Landau-theory does not apply,  $P_L(m)$  has a nontrivial (double peaked) shape [22,23]. While the theory of wedge wetting [24] explains some aspects of this transition, a full understanding is still lacking. No sharp transition is possible in the limit  $L_{\parallel} \rightarrow \infty$  at fixed area of the pore cross section: then only a rounded transition from a state where the interface is in the middle of the pore to finite-sized domains occurs.

Of course, in real systems many complications must be envisaged: e.g., confined fluids are off-lattice

systems, they lack the particle-hole symmetry implicit in the lattice gas already in the bulk. Treating such asymmetric off-lattice systems confined between walls presents particular challenges. A simple case will be dealt with in the next section.

### 3. Critical behavior of confined colloid-polymer mixtures

The simplest geometry of confinement assumes two equivalent parallel walls, i.e. a slit pore. This geometry may lead to “capillary condensation” [5–8,25]. A slightly undersaturated vapor can condense in small capillaries [26], but a quantitative experimental test of the theoretical predictions is difficult. E.g., the critical behavior should be that of the two-dimensional ( $2d$ ) Ising model [11], since the correlation length can show unlimited growth only in the two directions parallel to the walls. However, this  $2d$  critical behavior is visible only in an extremely narrow region around  $T_c(D)$ , except if the slit width  $D$  is of the order of a few particle diameters only. However, ideal and perfectly parallel walls so closely together are almost impossible to realize experimentally, for systems of small molecules. Here colloidal systems pose a distinct advantage, since colloidal particles have sizes in the  $\mu m$  range [27]. Colloid-polymer mixtures exhibit phase separation between a phase poor in colloids (“vapor”) and another phase rich in colloids (“liquid”) [28] in the bulk.

The salient features can be described by the simple Asakura-Oosawa (AO) model [29]. Colloids are modeled as hard spheres of diameter  $\sigma_c$  and polymers as soft spheres of diameter  $\sigma_p$ . The potential energy is infinite if two colloids or a colloid and a polymer overlap, but there is no energy cost when two polymers overlap. The control parameters are the colloid volume fraction  $\eta_c = \pi\sigma_c^3 N_c / (6V)$ , where  $N_c$  is the number of colloidal particles, and the fugacity  $z_p$  of the polymers. We use instead of  $z_p$  the related “polymer reservoir packing fraction”  $\eta_p^r = \pi z_p \sigma_p^3 / 6$  as a temperature-like variable.

For sufficiently large size ratios  $q \equiv \sigma_p / \sigma_c$  the AO model exhibits (purely driven by entropy) phase separation if  $\eta_p^r$  exceeds a critical value  $\eta_{p,cr}^r$ . Extensive grand-canonical Monte Carlo simulations in conjunction with finite size scaling have shown [30] that this model in the  $3d$  bulk exhibits critical exponents of the  $3d$  Ising universality class [11,16], as expected. In this study  $q = 0.8$  was used [30,31].

Fig. 5a) now shows [32] the order parameter  $\Delta$ ,

half the distance between the colloid packing fraction at the “liquid-like” ( $\eta_c^+$ ) and “vapor-like” ( $\eta_c^-$ ) branches of the coexistence curve in the  $(\eta_p^r, \eta_c)$  plane (Fig. 5b), for a thin slit,  $D = 5\sigma_c$ , plotted vs.  $\eta_p^r$ . The inset shows that  $\Delta$  can be obtained for two decades of  $t$ ,  $10^{-3} \leq t \leq 10^{-1}$ . The curvature on the log-log plot shows that the asymptotic  $2d$  behavior ( $\beta = 0.125$  [11]) is only reached extremely close to the critical point. Away from it, the effective exponent increases (but full  $3d$  critical behavior,  $\beta = 0.326$  [16], occurs only for much thicker slit pores - the confinement is already felt when the correlation length is about  $\xi \approx (D/2)\sigma_c = 2.5\sigma_c$ ).

We conclude by a discussion of the computational methods. The “raw data“ are generated by grand-canonical Monte Carlo (with the colloid fugacity  $z_c$  rather than  $\eta_c$  as an independent variable) for systems in a  $L \times L \times D$  geometry, with periodic boundary conditions in the  $(x, y)$  directions parallel to the walls. The first task is to find that  $z_c$  for which phase coexistence occurs, by “measuring” the probability distribution  $P_L(\eta_c | \eta_p^r, z_c)$  of  $\eta_c$ , at “inverse temperature”  $\eta_p^r$  and  $z_c$ .

Phase coexistence is established by tuning  $z_c$  such that  $P_L$  becomes bimodal (Fig. 6a), with two peaks of equal area [33,34]. The peak positions then yield the two branches of the coexistence curve  $\eta_c^-$ ,  $\eta_c^+$  in Fig. 6b).

While  $\eta_c$  in the regime of interest is not too large,  $0.1 \leq \eta_c \leq 0.4$ , the corresponding  $\eta_p$  is much larger (around  $\eta_p \approx 1$ ). As a consequence, standard grand-canonical Monte Carlo [19] would be extremely inefficient: almost all attempts to insert a colloid in such a dense system would fail [31]. This difficulty has been overcome by a newly invented cluster move [31].

However, when one samples a bimodal distribution with a huge free energy barrier  $F_L$  by straightforward Monte Carlo, one very rarely would obtain states near the minimum in Fig. 6a), and very seldomly transitions from one peak to the other one are sampled [35]. To find  $z_c$  one would need to sample many such transitions! This difficulty is overcome by “successive umbrella sampling” [36], a reweighting strategy designed for an efficient sampling of phase coexistence. Note, as an additional bonus, for  $L$  large enough one can extract from  $F_L$  the interfacial tension  $\gamma_L$  as  $\gamma_L = F_L / (2LD)$  [for  $L \rightarrow \infty$  near the minimum of  $k_B T \ln P$  in Fig. 6a) the state of the system is a colloid-rich domain, separated from the polymer-rich phase by two interfaces of area  $LD$ ] [32,35].

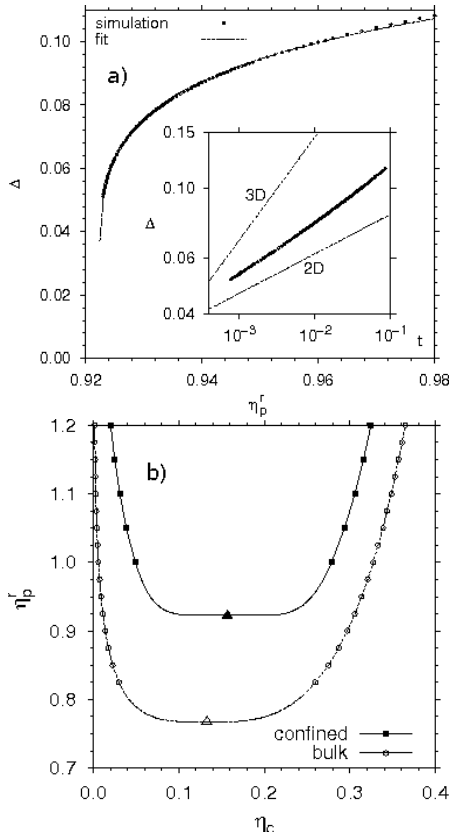


Fig. 5. (a) Order parameter  $\Delta$  as function of  $\eta_p^r$  for the confined AO model with  $q = 0.8$  and  $D = 5\sigma_c$ , using hard walls. The main frame shows  $\Delta$  in the thermodynamic limit on linear scales, the curve being a fit of the data to  $\Delta = \hat{B}_{\text{eff}} t^{\beta_{\text{eff}}}$ , yielding an “effective exponent”  $\beta_{\text{eff}} = 0.17$ , and  $\hat{B}_{\text{eff}} = 0.173$ ,  $\eta_{p,\text{cr}}^r = 0.9223$ . The inset shows the same data as a log-log plot vs.  $t = \eta_p^r / \eta_{p,\text{cr}}^r - 1$ . Broken straight lines indicate the slopes of the power laws for  $3d$  and  $2d$  behavior,  $\beta = 326$  [16] and  $\beta = 0.125$  [11]. (b) Coexistence curves of the AO model in the thermodynamic limit, for a bulk  $3d$  system and for a system in a slit of thickness  $D = 5\sigma$  with hard walls. Triangles mark the corresponding critical points; squares and circles are raw data obtained in the finite systems ( $L \times L \times L$  or  $L \times L \times D$ , respectively).

Finally, as Fig. 6b) shows for any finite  $L$  the two branches of the coexistence curve do not merge at the critical point (as they must do in the thermodynamic limit,  $L \rightarrow \infty$ , Fig. 5b), rather they “fan out” into the one-phase region,  $\eta_p^r < \eta_{p,\text{cr}}^r$  (this effect is an analog of the “finite size tails” familiar from the magnetization of Ising models, cf. e.g. Fig. 2(a)). So again a finite size scaling analysis is required, to achieve the extrapolation to the thermodynamic limit. However, this is more problematic than for standard critical phenomena [15,16,19]: the aspect ratio  $L/D$  enters as an additional variable [7,14,37].

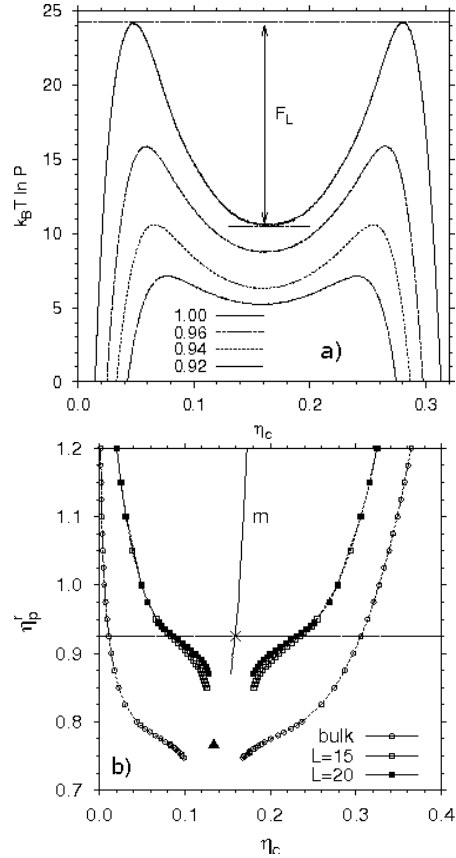


Fig. 6. (a): Logarithm  $k_B T \ln P_L$  of the confined AO model at phase coexistence, for  $q = 0.8$ ,  $D = 5\sigma_c$ ,  $L = 15\sigma_c$ , and 4 values of  $\eta_p^r$ , as indicated. For  $\eta_p^r$  distinctly larger than  $\eta_{p,\text{cr}}^r$  two peaks (representing the phase rich in polymers, left, and rich in colloids, right) are separated by a large free energy barrier  $F_L$ , as indicated for  $\eta_p^r = 1.0$ . (b) Coexistence curves of the confined AO model ( $D = 5\sigma_c$ ) and in the bulk, extracted from peak positions of distributions as shown in part a). Open circles show data for the  $3d$  bulk, the black triangle marks the critical point ( $\eta_c = 0.134$ ;  $\eta_p^r = 0.766$ ). The curve denoted as  $m$  shows the coexistence diameter ( $m = (\eta_c^+ + \eta_c^-)/2$ ) of the confined system with  $L = 20\sigma_c$ . The cross (and horizontal line) highlights  $\eta_{p,\text{cr}}^r$ . Open and closed squares show  $\eta_c^+$ ,  $\eta_c^-$  for the confined system for two lateral dimensions  $L$  (in units of  $\sigma_c$ ).

Analyzing intersections of the “cumulant”  $U_4 = \langle M^2 \rangle^2 / \langle M^4 \rangle$  where  $M = \eta_c - \langle \eta_c \rangle$  as function of  $\eta_p^r$  for various  $L$  one does not find a unique intersection. Rather these intersections are scattered [32] (only for  $L/D \rightarrow \infty$  the unique intersection point of the  $2d$  Ising universality class will be recovered). Progress was then obtained [32] by applying a novel extension [38] of finite size scaling that is not biased by any assumptions on critical exponents. This method then has allowed to study the smooth change of the effective exponent with the distance  $t$

[insert of Fig. 5a)].

This is not the whole story on confined colloid-polymer mixtures: interesting aspects also concern the test [39] of the predictions [5] on the shift of phase equilibria and critical points with thickness  $D$ , etc.

#### 4. Concluding remarks

In this paper, examples have been discussed which show that the statistical mechanics of a system under nanoscopic confinement poses challenging problems.

Monte Carlo is the method of choice for such problems, but studies require both a careful choice of the algorithm, suitably adapted to the model, and a state of the art analysis of the simulation data. A basic strategy is to study how properties change when linear dimensions of the system are varied. Powerful finite size scaling “tools” exist to analyze the “raw data”. Colloid-polymer mixtures are an example to show that progress results not just from “brute force”, but from careful improvements of the simulation algorithm (such as “cluster moves” [31], “successive umbrella sampling” [36], etc.). Statistical mechanics of condensed matter is still very rich offering many interesting problems where such approaches are useful.

#### Acknowledgements

The research reviewed here has been supported by the Deutsche Forschungsgemeinschaft (grants No 436 BUL 113/130 and TR6/A5).

#### References

- [1] A. Milchev et al., *Europhys. Lett.* 70 (2005) 348.
- [2] A. Milchev et al., *Phys. Rev. E* 72 (2005) 031603.
- [3] K. Binder, P.C. Hohenberg, *Phys. Rev. B* 6 (1972) 3461; *ibid* B9 (1974) 2192.
- [4] K. Binder, in: C. Domb, J.L. Lebowitz (Eds.), *Phase Transitions and Critical Phenomena*, Vol 8, Academic, London, 1983, p. 1.
- [5] M.E. Fisher, H. Nakanishi, *J. Chem. Phys.* 75 (1981) 5857; H. Nakanishi, M.E. Fisher, *ibid* 78 (1983) 3279.
- [6] K. Binder, D.P. Landau, *J. Chem. Phys.* 96 (1992) 1444.
- [7] O. Dillmann, W. Janke, M. Müller, K. Binder, *J. Chem. Phys.* 114 (2001) 5853.
- [8] K. Binder, D.P. Landau, M. Müller, *J. Stat. Phys.* 110 (2003) 1411.
- [9] K. Binder, D.P. Landau, A.M. Ferrenberg, *Phys. Rev. Lett.* 74 (1995) 298; *Phys. Rev. E* 51 (1995) 2823.
- [10] K. Binder, R. Evans, D.P. Landau, A.M. Ferrenberg, *Phys. Rev. E* 53 (1996) 5023.
- [11] M.E. Fisher, *Rev. Mod. Phys.* 46 (1974) 587.
- [12] M.E. Fisher, in: M.S. Green (Ed.), *Critical Phenomena*, Academic, London, 1971, p. 1.
- [13] V. Privman (Ed.) *Finite Size Scaling and the Numerical Simulation of Statistical Systems*, World Scientific, Singapore, 1990.
- [14] K. Binder, in: H. Gausterer, C.B. Lang (Eds.) *Computational Methods in Field Theory*, Springer, Berlin, 1992, p. 59.
- [15] K. Binder, *Z. Phys. B: Condens. Matter* 43 (1981) 119.
- [16] K. Binder, E. Luijten, *Phys. Rep.* 344 (2001) 159.
- [17] E. Brézin, J. Zinn-Justin: *Nucl. Phys. B* 257 (1985) 867.
- [18] A.O. Parry, A.J. Wood, C. Rascon, *J. Phys.: Condens. Matter* 13 (2001) 4591.
- [19] D.P. Landau, K. Binder, *A Guide Monte Carlo Simulations in Statistical Physics*, 2nd Ed., Cambridge University Press, Cambridge, 2005.
- [20] J.O. Indekeu, *Int. J. Mod. Phys. B* 138 (1994) 309.
- [21] M. Hasenbuch, K. Pinn, *Physica A* 203 (1994) 189.
- [22] A. Milchev, M. Müller, K. Binder, D.P. Landau, *Phys. Rev. Lett.* 90 (2003) 136101.
- [23] A. Milchev et al., *Phys. Rev. E* 68 (2003) 031601.
- [24] A.O. Parry et al., *Phys. Rev. Lett.* 83 (1999) 5535.
- [25] L.D. Gelb, K.E. Gubbins, R. Rahakrishnan, M. Sliwinski-Barthowiak, *Rep. Progr. Phys.* 62 (1999) 1573.
- [26] W.T. Thomson (Lord Kelvin), *Philos. Mag.* 42 (1871) 448.
- [27] H. Löwen, *J. Phys.: Condens. Matter* 13 (2001) R415.
- [28] W. Poon, *J. Phys.: Condens. Matter* 14 (2002) R589.
- [29] S. Asakura, F. Oosawa, *J. Chem. Phys.* 22 (1954) 1255.
- [30] R.L.C. Vink, J. Horbach, K. Binder, *Phys. Rev. E* 71 (2005) 011401; *J. Chem. Phys.* 122 (2005).
- [31] R.L.C. Vink, J. Horbach, *J. Chem. Phys.* 121 (2004) 3253; *J. Phys.: Condens. Matter* 16 (2004) S3807; R.L.C. Vink, *cond-mat/0402585*.
- [32] R.L.C. Vink et al., *Phys. Rev. E* 73 (2006) 056118.
- [33] K. Binder, D.P. Landau, *Phys. Rev. B* 30 (1984) 1477.
- [34] C. Borgs, R. Kotecky, *J. Stat. Phys.* 61 (1990) 79.
- [35] K. Binder, *Phys. Rev. A* 25 (1982) 1699.
- [36] P. Virnau, M. Müller, *J. Chem. Phys.* 120 (2004) 10925.
- [37] K. Binder, J.S. Wang, *J. Stat. Phys.* 35 (1989) 87.
- [38] Y.C. Kim et al., *Phys. Rev. Lett.* 91 (2003) 065701.
- [39] R.L.C. Vink et al., *Phys. Rev. E*, accepted for publication (2006); preprint *cond-mat/0607086*.